Single-kink dynamics in a one-dimensional atomic chain: A nonlinear atomistic theory and numerical simulation

J. Andrew Combs and Sidney Yip
Department of Nuclear Engineering, Massachusetts Institute of Technology, Cambridge, Massachusetts 02139
(Received 8 April 1983)

A nonlinear lattice-dynamical theory of single kinks is presented which involves a simple equation of constraint. A set of coupled equations of motion is derived for the kink and discrete lattice fluctuations, which retains the full details of their mutual interaction. The theory is used to study ϕ^4-lattice kinks. For low kink velocities the kink equation of motion reduces to a generalized Langevin form. The static kink energy is found to vary periodically with the lattice spacing, implying that thermal kink motion is an activation process at low temperatures. Numerical studies reveal that kinks undergo damped motion, oscillatory motion, and trapping between lattice sites. Damping and oscillatory motion vanish as the continuum limit is approached. A phenomenological theory of damped kink propagation is developed and compared with numerical simulation.

I. INTRODUCTION

A great deal of attention has been devoted to the study of soliton, kink, and other solitary-wave motions in one-dimensional systems. Dislocation kinetics have been modeled by solitary waves[1,2] in the past. The Frenkel-Kontorowa model[3] of dislocations is a well-known example. More recently, Krumhansl and Schrieffer[4] proposed that the motions of solitary waves called kinks or domain walls are responsible for the extremely narrow central peak observed near ferroelectric structural phase transitions. Their work has stimulated much interest in the investigation of kinks and domain walls,[5–20] and the applications of solitary-wave models to other phenomena such as charge-density waves in polymer chains[21] and dielectric relaxation.[22,23]

Virtually all one-dimensional studies of lattices that support solitary waves use some variation of the following Hamiltonian form:

$$H=\sum_l \frac{m\dot{u}_l^2}{2}+\sum_\lambda \frac{C}{2}(u_{l+1}-u_l)^2+\sum_l V_R(u_l)+H_{\rm ext}\ . \tag{1.1}$$

$u_l(t)$ is the displacement of the lth atom of mass m from its equilibrium lattice site $x(l)=lb$, b is the lattice constant, C is the attractive Hooke's-law force constant which couples near neighbors, $H_{\rm ext}$ represents a coupling to an external field, and $V_R(u_l)$ is a rigid-lattice single-particle potential. The most common choices for V_R are the bistable ϕ^4 potential

$$V_r(u_l)=-\frac{A}{2}u_l^2+\frac{B}{4}u_l^4 \tag{1.2}$$

and the sine-Gordon (SG) potential,

$$V_R(u_l)=\frac{\tilde{E}_0}{2}[1-\cos(\alpha_0 u_l)]\ , \tag{1.3}$$

which are depicted in Fig. 1.

At low system energies, particles like to oscillate about the bottom of one well or another. The Hooke's-law coupling tends to minimize deviations of near-neighbor bond lengths from the lattice spacing b. This, in turn, tends to minimize the energy. Particles of the chain will, therefore, tend to align themselves in the same well as their near neighbor. This will lead to a situation where entire segments (or domains) of the chain will be aligned or ordered. But thermal fluctuations will tend to maximize entropy, thus disturbing this order. Usually, therefore, two domains whose atoms occupy different walls find themselves neighboring one another. The transition region between the domains is a wall-like structure or kink in the atomic displacement profile (see Fig. 2). It is a stable solitary wave connecting the different domains, and is appropriately named a kink or domain wall.

One of the most significant properties of kinks is that they are mobile. They move in response to thermal fluctuations[13,14] and external stresses,[1,12,15] causing the expansion or contraction of the domains which they bound. Because of this, kinks have significant nonlinear transport

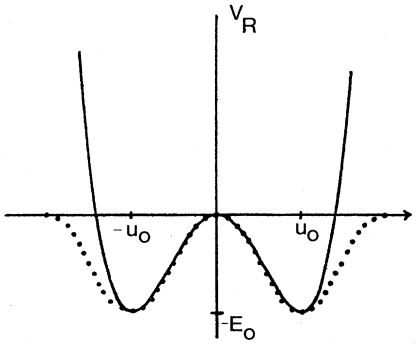

FIG. 1. Rigid-lattice single-particle potentials V. The solid line is the ϕ^4 potential; the dotted line is the SG potential. $u_o=(|A|/B)^{1/2}$ and π/α_0, $E_0=A^2/4B$ and $\tilde{E}_0$ for the ϕ^4 and SG potentials, respectively (see text).

properties.[15] Kink kinetics in ferroelectrics have a significant effect on switching times, hystereses, and stability in optical switching and memory devices.[11]

Past attempts to study one-dimensional lattice kinks have included linear models to dislocations[1,2] in the analysis of dislocation-fluctuation coupling of dislocations to acoustical radiation. More recent attempts have made use of a continuum approximation to (1.1) with (1.2), reducing the problem to a nonlinear-field theory of kink motions.[8,9,12,16] In each of the latter cases attempts were made to obtain an equation of motion for the kink of the form $Ma=f$, where M is a kink effective mass and a is the kink acceleration. The forces on the kink consist of kink-fluctuation interactions or external fields.

The progress in the theory of lattice kinks has not been altogether satisfactory. Formulations of kink dynamics that have used the continuum approach yield predictions of kink motion that vary substantially[4,9,12,16] with respect to kink diffusion and kink-phonon interactions. The kink diffusion constant in the ϕ^4 lattice, for example, is predicted to diverge,[12] depend upon temperature T^2 (Ref. 16) but not upon the Hooke's-law coupling parameter C, and upon $T^{1/2}$ and C to a power.[19] These differences are due primarily to a lack of a common understanding of how to calculate the forces introduced by kink-fluctuation interactions in the continuum approximation. The continuum theory itself suffers from an intrinsic weakness in that it ignores the discrete effects of the lattice. Lattice trapping effects, for example, found by the authors (Sec. II) and others[10] are not present in the traditional continuum approach. In addition, our studies show that kink-fluctuation coupling is largely a discrete lattice effect. Because of the power of the continuum approach it would be very useful to be able to incorporate the most important effects of lattice discreteness into a new continuum theory of kink motion.

In this paper we propose a nonlinear theory of lattice dynamics of single kinks which is generally applicable to all Hamiltonians of the form (1.1) that support solitary waves. It is a reformulation of the lattice dynamics of the N particle chain in terms of N fluctuations and a single kink, an equivalent $(N+1)$-body problem. Central to this theory is the proposal of a simple equation of constraint which determines the kink position. The equation of constraint and the N equations of motion for the atomic displacements obtained from (1.1) are used to derive a coupled set of Newton's laws for the kink and fluctuation motions. The full detail of the interaction of the lattice kink with discrete fluctuations is retained without using the continuum approach. A continuum approximation can be made, however, which gives rise to terms directly attributable to the effect of lattice discreteness upon kink structure.

We apply our theory to the case of the ϕ^4 potential (1.2) in the absence of external fields; thus

$$H=\sum_l \frac{m\dot{u}_l^2}{2}+\sum_l \left[\frac{C}{2}(u_{l+1}-u_l)^2-\frac{A}{2}u_l^2+\frac{B}{4}u_l^4\right] . \tag{1.4}$$

We study kink structure and dynamics both analytically and numerically. In Sec. II we present a review of the basic ideas of solitons in the traditional continuum approach, including the linear perturbation analysis. In Sec. III we present the kink-fluctuation theory.

It is found that for low kink velocities the kink equation of motion reduces to a generalized Langevin form. A continuum approximation is made which retains the effects of the large amplitude kink structure exactly, thereby giving rise to "discrete" effects not present in the traditional continuum approach. The new continuum theory is, therefore, more exact than the traditional continuum approach since approximations are made only in small amplitudes. A comparison with other kink equations of motion is made.

In Sec. IV the static structure of the kink is analyzed using the equations derived in Sec. III, using both the approximate continuum approach and an exact numerical solution. It is found that the static kink energy undergoes a variation in the potential energy periodic in the lattice spacing, thereby giving rise to a periodic kink potential. This suggests that in a thermal lattice kink motion is an activation process. The latter observation has important implications for diffusive behavior and the central peak phenomenon, topics treated in a subsequent paper.

In Sec. V, with the aid of numerical solutions of the lattice equations of motion, kinks are found to undergo damped motion, oscillatory motion, and trapping between lattice sites. Because of the complexity of the kink-fluctuation interaction, a phenomenological approach to characterize the damping is made by numerically "measuring" the damped constant. A phenomenological theory of damped kink propagation is, therefore, developed and compared to the numerical simulation results. Such a phenomenological approach leads naturally to a stochastic model of thermal kink behavior.[24]

II. CONTINUUM DESCRIPTION AND LINEAR PERTURBATION ANALYSIS

We consider a chain of atoms, which execute one-dimensional motions which are purely longitudinal (or purely transverse) relative to the chain direction. The equation of motion derived from (1.4) is

$$m\frac{\partial^2 u_l(t)}{\partial t^2}-C[u_{l+1}(t)+u_{l-1}(t)-2u_l(t)]+\frac{\partial V_R}{\partial u_l}=0 . \tag{2.1}$$

For the ϕ^4 potential (2.1) can be cast into the nondimensional form,

$$\frac{\partial^2 u_l(t)}{\partial t^2}-C[u_{l+1}(t)+u_{l-1}(t)-2u_l(t)]-u_l(t)+u_l^3(t)=0 , \tag{2.2}$$

where the dimensionless quantities are $u_l'=u_l(B/|A|)^{1/2}$, $t'=t(|A|/m)^{1/2}$, and $C'=C/A$; all the quantities in (2.2) are dimensionless and the primes have been suppressed. Unless otherwise stated, all subsequent quantities are expressed as nondimensional numbers.

the following (2.2) will be called the ϕ^4-lattice equation.

The continuum description of the ϕ^4 lattice follows from the replacement of the discrete coordinate $u_l(t)$ by the displacement field $u(x,t)$, and the approximation

$$u_{l+1}+u_{l-1}-2u_l \simeq b^2 \frac{\partial^2 u}{\partial x^2} \ . \tag{2.3}$$

Then (2.2) becomes the ϕ^4-continuum equation

$$\frac{\partial^2 u(x,t)}{\partial t^2}-c_0^2\frac{\partial^2 u(x,t)}{\partial x^2}-u(x,t)+u^3(x,t)=0 \ , \tag{2.4}$$

with $c_0^2=C$. The continuum description serves as a useful reference system for the analysis of kink motions in a discrete lattice. There are a number of properties of (2.4) which should be noted before starting a discussion of discrete lattice effects.

Inspection of the homogeneous equation (2.4) shows that trivial solutions exist with $u=\pm 1.0$, which correspond to all the particles sitting at the position of one of the potential minima. These solutions are stable. Another trivial solution is $u=0$, which is unstable because the particles then are sitting at the top of the energy barrier. Expanding about $u=1$ and linearizing, one obtains the Klein-Gordon equation,

$$\frac{\partial^2 \eta(x,t)}{\partial t^2}-c_0^2\frac{\partial^2 \eta(x,t)}{\partial x^2}+\omega_0^2\eta(x,t)=0 \ , \tag{2.5}$$

for small fluctuations $\eta(x,t)$, with $\omega_0^2=2$. The dispersion relation corresponding to traveling wave solutions,

$$\eta_q(x,t)=\alpha_q \sin(qx+\omega t) \ , \tag{2.6}$$

is

$$\omega_q^2=\omega_0^2+c_0^2q^2 \ . \tag{2.7}$$

This shows that (2.5) describes the system as simply a set of coupled oscillators with each oscillator subjected to an additional linear restoring force with characteristic frequency ω_0. From the standpoint of discussing kink motions, equations such as (2.5) are of limited interest.

Equation (2.4) itself admits wave solutions of the form

$$u_K(x-X)=\pm\tanh[K(x-X)] \ . \tag{2.8}$$

If K and X are treated as constants, then substitution of (2.8) into (2.4) gives the relation $K^2=1/2C=1/2c_0^2$, and X can be any arbitrary constant. Figure 2 shows a plot of (2.8) superimposed upon a typical thermal-lattice profile; it is seen that $u_K(x-X)$ describes a kink configuration with K and X determining, respectively, the width and position of a stationary kink. Since we are interested in moving kinks, we can replace the constant X in (2.8) by

$$X(t)=X_0+Vt \ , \tag{2.9}$$

where X_0 is the initial position and V is the constant speed of the kink. Then K becomes

$$K=K_0\gamma \ , \tag{2.10}$$

with $K_0^2=1/2C$ and $\gamma=1/(1-V^2/c_0^2)^{1/2}$. Notice that γ is just the Lorentz contraction factor which arises from the Lorentz invariance of (2.4). Equation (2.8) describes a solitary wave which exists in the ϕ^4-continuum description. In a dynamic lattice one needs to consider the interaction of this wave with fluctuations in the system.

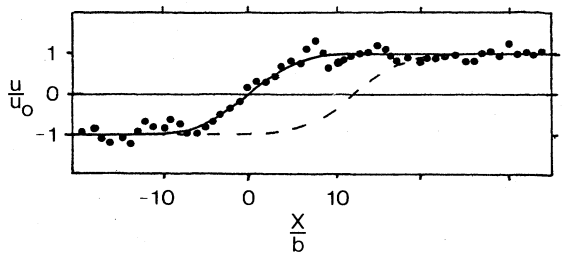

FIG. 2. Typical picture of a ϕ^4 lattice (dotted line) in the vicinity of a lattice kink when $C=1$. Fluctuations in the atomic displacements from their equilibrium positions x occur about the solid line obtained from Eq. (2.8) with $X=0$. This curve is a continuum kink. In general, a kink is not stationary; the dashed curve is obtained by a translation of a continuum kink to the right by ten lattice spacings.

A perturbation theory approach to the analysis of kink-fluctuation interactions begins with the decomposition,

$$u(x,t)=u_K(x-X(t))+\psi(x-X(t),t) \ , \tag{2.11}$$

where the fluctuation ψ is assumed to be small in comparison to u_K. Inserting this into (2.4), keeping only terms linear in ψ, and performing a Lorentz transformation to the moving coordinate system where the kink is stationary, one finds

$$\frac{\partial^2 \psi(x,t)}{\partial t^2}-c_0^2\frac{\partial^2 \psi(x,t)}{\partial x^2}+V_S(x-X_0)\psi(x,t)=0 \ , \tag{2.12}$$

where

$$V_S(x)=3u_K^2(x)-1 \tag{2.13}$$

may be regarded as the scattering potential due to the presence of a stationary kink. The eigenvalue problem resulting from the assumption of sinusoidal solutions of the form $\psi \sim A(x)e^{i\omega t}$ has already been analyzed.[16] The eigenvalue spectrum consists of two discrete modes, $\omega_T=0$, $\omega_L=(\frac{3}{2})^{1/2}$, and a continuum of modes $\omega_0<\omega_q<(\omega_q^2+\pi c_0^2)^{1/2}$; the corresponding eigenfunctions $y_T(x)$, $y_L(x)$, and $y_q(x)$ are known analytically. Thus

$$\psi(x,t)=\alpha_T y_T(x)+\alpha_L y_L(x)e^{i\omega_L t}+\int dq\, \alpha_q y_q(x)e^{i\omega_q t} \ . \tag{2.14}$$

The linear theory represented by (2.12) shows that the stationary kink is absolutely stable to fluctuations y_L and y_q, and neutrally stable to y_T. The traveling fluctuations simply suffer a phase shift upon passing through the kink. Thus, to first order in the fluctuations, continuum kinks move freely, uniformly, and without acceleration.

One expects the continuum description to be valid for large values of C, since the kink width K varies inversely with C, and a large kink width means small displacement gradients and higher derivatives [cf. (2.3)]. To determine

the extent of its validity we solve the perturbation theory (2.11)—(2.14) analytically and the ϕ^4-lattice equations (2.2) numerically for the case of a single propagating kink. With one exception, we restrict our attention to initial conditions in which atomic motions are purely due to the movement of the kink, i.e., $\psi_l(0)=\dot{\psi}_l(0)=0$, $u_l(0)=u_K^l(X(0))$, $\dot{u}_l(0)=-V(0)\partial u_K^l/\partial X$. In this case the continuum solution is particulary simple: The kink propagates at a constant velocity [see (2.8) and (2.9)] and the fluctuations remain zero [since there is no source term in (2.12)]. The reader is referred elsewhere for studies of more general initial conditions.[24] Figure 3 shows space-time evolutions of single kinks whose initial positions and velocities in a 100-atom lattice are $X=50.5$ and $V=3$; the value of C is reduced from 20 to 10 to 5 in Figs. 3(a), 3(b), and 3(c), respectively. In Fig. 3(a) the kink profile is essentially undistorted and the velocity remains steady. Thus in this case the continuum approximation is valid. In Fig. 3(b) the kink dissipates energy by radiating fluctuations behind the kink. Deviations from the continuum theory are perceptable, even on the rough scale of the graph. In Fig. 3(c) strong dissipation and large fluctuations are present; however, in this case the initial condition included nonzero values of the fluctuation displacements and velocities which lead to a large initial radiation pulse. Figure 4 continues to show that as C decreases kink propagation no longer behaves according to the continuum theory. At $C=1$ the kink velocity decreases with time in an oscillatory manner. At still smaller C the kink not only will slow down but it can be trapped, as shown in Fig. 5. The processes of kink damping and trapping do not follow from the linear-perturbation analysis of the ϕ^4-continuum equation. Their manifestations are the results of strong kink-fluctuation interactions. As we will see below, the origin of such couplings lies in discrete lattice effects, namely, the difference between (2.2) and (2.4).

III. REFORMULATION OF KINKS AND FLUCTUATIONS

In order to analyze kink damping and trapping processes it is clearly essential to take into account kink-fluctuation interactions. We now consider a reformulation of the problem based on a decomposition of the discrete displacment $u_l(t)$ in a manner similar to (2.11):

$$u_l(t)=u_K^l(X(t))+\psi_l(t)\ , \tag{3.1}$$

where $u_K^l(X(t))=\tanh K(x_l-X(t))$. The reference system in this case is a kink whose position $X(t)$ will be treated as a dynamical variable. The width K also can be generalized, but for simplicity we will assign to it the static value $K=K_0=1/\sqrt{2C}$. To determine $X(t)$ a condition of constraint needs to be invoked. We will adopt

$$\sum_l \frac{\partial u_K}{\partial X}\bigg|_{x=x_l}=0\ . \tag{3.2}$$

This is a reasonable choice since it tends to minimize ψ_l in the domain-wall region (where $\partial u_K/\partial x$ peaks). It has been used previously in the study of ϕ^4-field theory.[25]

Substitution of (3.1) into (2.2) yields

$$\frac{\partial^2\psi_l}{\partial t^2}-C(\psi_{l+1}+\psi_{l-1}-2\psi_l)+\frac{\partial^2 u_K}{\partial t^2}-C(u_K^{l+1}+u_K^{l-1}-2u_K)+\frac{\partial V_R}{\partial u_l}\bigg|_{u_l=u_K^l+\psi_l}=0\ . \tag{3.3}$$

The term representing the dispersion force can be written as

$$C(u_K^{l+1}+u_K^{l-1}-2u_K)=c_0^2\frac{\partial^2 u_K}{\partial x^2}+F_K^l(X)\ , \tag{3.4}$$

where

$$F_K^l(X)=\sum_{j=2}^{\infty}\frac{2c_0^2}{(2j)!}\frac{\partial^{2j}u_K}{\partial x^{2j}}\bigg|_l \tag{3.5}$$

represents the discrete lattice effects associated with the kink structure. Using (3.5) one can evaluate the spatial variation of F_K and its dependence on C. Numerical computations show that the series is strongly convergent for

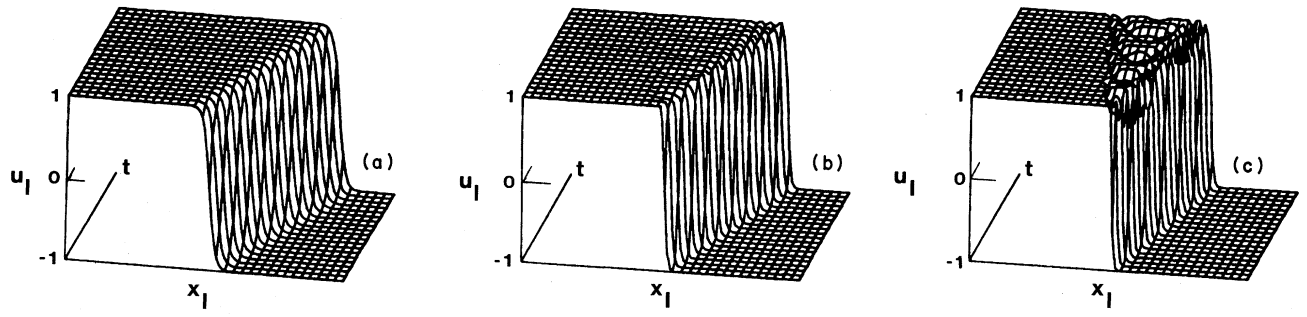

FIG. 3. Space-time evolution of atomic amplitudes obtained by numerical integration of (2.2). The initial conditions for (a) and (b) are a moving kink (2.8) with $\psi(x,0)=0.0$ where $V(0)=3$ and C is varied. (a) $C=20$. Velocity is constant at its initial value. Fluctuations cannot be seen. No discernable difference exists between this solution and the continuum solution. (b) $C=10$. Velocity is reduced to roughly 2.5. A small fluctuation wake appears behind the kink. (c) $C=5$. Fluctuation amplitudes and displacements were nonzero initially about the kink position. The velocity drops to 1.5 and a fluctuation wake of sizable amplitude develops behind the kink.

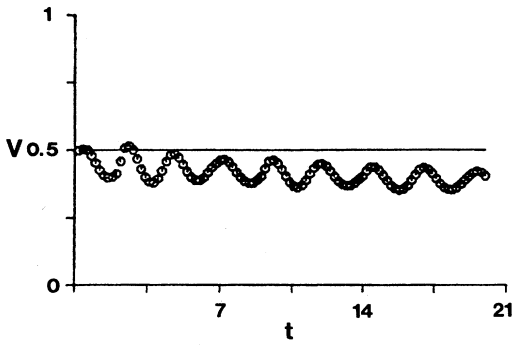

FIG. 4. Lattice kink velocity V (open circles) compared with the continuum solution (2.4) (solid line) for $C=1$. The lattice kink velocity is determined by finite difference of $X(t)$, which in turn is obtained from (3.1) and (3.2).

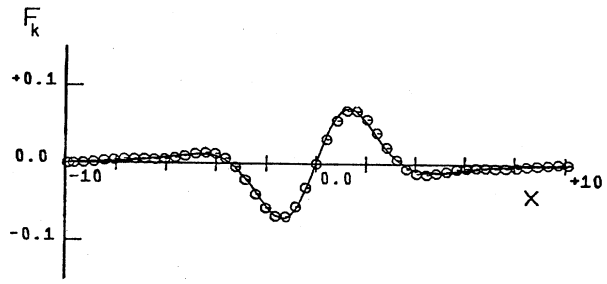

FIG. 6. F_k for $C=0.75$ as a function of distance x from the kink position $X=0.0$. The circles are obtained from (3.5) by truncating at the tenth term; the solid line is just the left-hand side of (3.4) minus the first term on the right-hand side. Thus F_k is just the difference of the lattice and continuum approximation dispersion forces due to the presence of a kink.

$C>0.6$. Figure 6 shows that $F_K(x-X)$ is odd about X and more or less localized about $x=X$. Figure 7 shows that the maximum value of F_K decreases with C. In general one knows that

$$\lim_{c\to\infty} F_K=0 \tag{3.6}$$

since in this limit the width becomes very large and all higher-order derivatives must vanish. Thus in the continuum limit F_K vanishes.

Using (3.4) and the identity

$$-c_0^2\frac{\partial^2 u_K}{\partial x^2}\bigg|_l+\frac{\partial V_R}{\partial u}\bigg|_{u=u_K^l}=0\ , \tag{3.7}$$

one obtains from (3.3) an equation of motion for the fluctuation amplitudes ψ_l,

$$\frac{\partial^2\psi_l}{\partial t^2}-C(\psi_{l+1}+\psi_{l-1}-2\psi_l)+F_{K\psi}^l[u_K,\psi]=F_K^l-\frac{\partial^2 u_K^l}{\partial t^2}\ , \tag{3.8}$$

where $F_{K\psi}^l$ is a kink-fluctuation interaction,

$$F_{K\psi}^l[u_K,\psi]=\frac{\partial V_R}{\partial u}\bigg|_{u_K^l+\psi_l}-\frac{\partial V_R}{\partial u}\bigg|_{u_K^l}\ . \tag{3.9}$$

The two terms on the right-hand side of (3.8) play the role of source terms, the first arising from kink structure and the second from kink acceleration.

Thus far the kink position X in u_K^l is still unspecified. We obtain the equation of motion for $X(t)$ by taking the second derivative of (3.2) (see Appendix) to yield

$$M(t)\ddot{X}(t)+\lambda(t)\dot{X}(t)+\zeta(t)\dot{X}^2(t)=-\frac{\partial U}{\partial X}\ , \tag{3.10}$$

where, letting $u_K'=-K^{-1}\partial u_K/\partial X$,

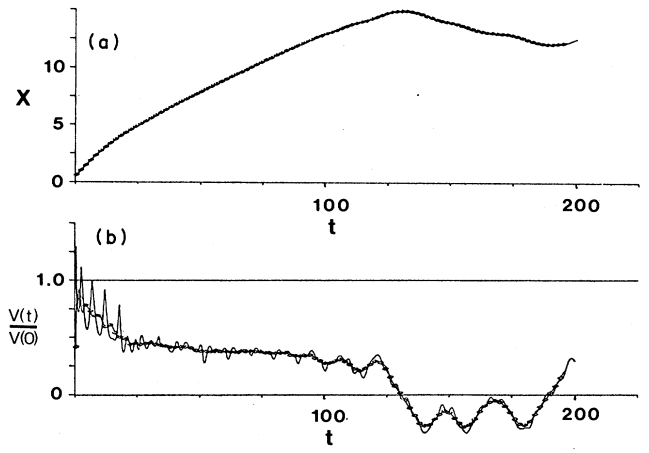

FIG. 5. (a) Kink trajectory in units of the lattice spacing b for $C=0.7$ and $V(0)=0.28$. Notice that kink initially moves forward, then turns around to move backward after about 15 lattice spacings. (b) The ratio of the kink velocity to the initial kink velocity. Solid line represents the instantaneous value $\dot{X}(t)$ while the connected diamonds represent a time average over the interval $(t-2,t+2)$.

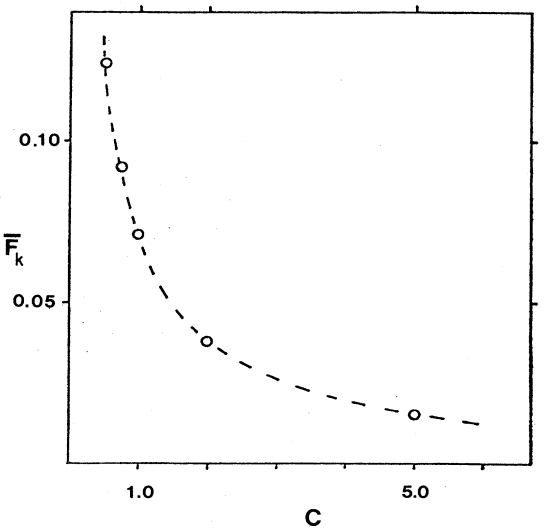

FIG. 7. Maximum amplitude $\bar{F}_k$ of F_k is plotted vs C. The dashed line is drawn as a guide to the eye.

$$M=\sum_l K^2(u_K')_l^2-\sum_l K^2(u_K'')_l \ , \tag{3.11}$$

$$\lambda=-2\sum_l K^2(u_K'')_l\dot{\psi}_l \ , \tag{3.12}$$

$$\zeta=-\sum_l K^3(u_K'u_K'')_l+\sum_l K^3(u_K''')_l\psi_l \ , \tag{3.13}$$

$$U=\sum_l \frac{C}{2}(u_{l+1}-u_l)^2+\sum_l V_R(u_l) \ . \tag{3.14}$$

It turns out that the $\dot{X}^2$ term is quite small except when $V\sim c_0$, so that (3.10) is of the form

$$M(t)\ddot{X}(t)+\lambda(t)\dot{X}(t)=-\frac{\partial U}{\partial X} \ , \tag{3.15}$$

which is the equation of motion of a particle of mass M moving in a medium characterized by a friction coefficient $\lambda(t)$ and under the influence of a potential U. It should be noted that M and U are functions of $\psi_l(t)$ as well as $u_K^l(X)$. But, in cases where $\psi_l \ll u_K^l$, M is roughly constant ($\simeq M_0$, say) and, as will be seen in the next section, U is roughly periodic in X with the periodicity of the lattice spacing b. Thus, it is appropriate to separate U into $U=U_K(X)$ only, and a fluctuation part $R(t)$ as follows:

$$M_0\ddot{X}(t)+\lambda(t)\dot{X}(t)=R(t)-\frac{\partial U_K}{\partial X} \ . \tag{3.16}$$

This is a generalized Langevin equation; if $\langle\lambda\rangle<0$ then the $\lambda(t)\dot{X}$ term is a damping term. Equation (3.16) strongly suggests that the kink is a Langevin- or Brownian-type particle in a thermal lattice as has been hypothesized elsewhere.[13]

Equation (3.8) is an equation for ψ_l in a discrete lattice. It is useful to examine the corresponding continuum description. Replacing $\psi_l(t)$ by the fluctuation field $\psi(x,t)$ and applying the same approximation as (2.3) one finds

$$\ddot{\psi}-c_0^2\frac{\partial^2\psi}{\partial x^2}+F_{K\psi}[u_K,\psi]=F_K-\ddot{u}_K \ , \tag{3.17}$$

where we have replaced u_K^l by u_K. This result can be expressed as an equation for the displacement field

$$u(x,t)=u_K(x-X(t))+\psi(x,t) \tag{3.18}$$

and one obtains

$$\ddot{u}-c_0^2\frac{\partial^2 u}{\partial x^2}+\frac{\partial V_R}{\partial u}=F_K(x-X) \ . \tag{3.19}$$

Comparison of (3.19) with (2.4) shows that the source term F_K is entirely missing in the latter. The appearance of F_K in (3.19) results in an extended continuum description which takes into account the discrete lattice effects associated with kink structure. Because the approximation (2.3) was applied only to the fluctuations and not to the kink, the higher-order spatial derivatives of u_K are retained. Since F_K vanishes in the large-C limit, the conventional continuum description (2.4) is recovered from (3.19).

The continuum approximation can also be made for the kink equations (3.10)—(3.14). In particular, let

$$M\to M_K-\int dx\, K^2u_K''\psi\equiv M_K+\tilde{M} \ ,$$

$$M_K\equiv\int dx\, K^2(u_K')^2=\frac{2\sqrt{2}}{3\sqrt{C}} \tag{3.20}$$

$$\lambda\to -2\int dx\, K^2u_K''\dot{\psi}\equiv\lambda_c \ , \tag{3.21}$$

$$\zeta\to\int dx\, K^3u_K'''\equiv\zeta_c \ , \tag{3.22}$$

$$-\frac{\partial U}{\partial X}=-\sum_l K(u_K')_l\frac{\partial U}{\partial u_l}$$

$$\to-\int dx\, Ku_K'\frac{\partial U}{\partial u}$$

$$=-\int dx\, Ku_K'\left[-c_0^2\frac{\partial^2 u}{\partial x^2}+\frac{\partial V_R}{\partial u}\right] . \tag{3.23}$$

At low velocity, the ϕ^4 field yields

$$-c_0^2\frac{\partial^2 u_K}{\partial x^2}+u_K-u_K^3=0 \ .$$

Then

$$-\frac{\partial U}{\partial X}\to-\int dx\, Ku_K'\left[-c_0^2\frac{\partial^2\psi}{\partial x^2}+(3u_K^2-1)\psi+3u_K\psi^2+\psi^3\right] ,$$

or

$$(M_K+\tilde{M})\ddot{X}+\lambda_c\dot{X}+\zeta_c\dot{X}^2$$

$$=-\int dx\, Ku_K'\left[-c_0^2\frac{\partial^2\psi}{\partial x^2}+(3u_K^2-1)\psi+3u_K\psi^2+\psi^3\right] . \tag{3.24}$$

This should be compared with Sahni and Mazenko's[8] equation,

$$M_K\ddot{X}=-\int dx\, Ku_K'[(3u_K^2-1)\psi+3u_K\psi^2+\psi^3] \ . \tag{3.25}$$

Their equation is not necessarily incorrect; the kink equations (3.8)—(3.10) are derived from a postulated equation of constraint which is not unique.

Another equation of kink motion was attempted by Wada and Schrieffer.[16] They place no constraint upon ψ, except that the motion of the kink is determined from a finite-amplitude perturbation theory in the amplitudes of the fluctuations ψ. In particular, taking an initial kink position X_0, ψ is to be determined from

$$\ddot{\psi}-c_0^2\frac{\partial^2\psi}{\partial x^2}+(3u_K^2-1)\psi+3u_K\psi^2+\psi^3=0 \tag{3.26}$$

and $X(t)$ from

$$X(t)=X_0+\text{const}\times\alpha_T(t) \ , \tag{3.27}$$

where $\alpha_T(t)$ is the zero-frequency mode amplitude discussed in Sec. II. Thus

$$\ddot{X}(t)=\text{const}\times\ddot{\alpha}_T(t)\ . \tag{3.28}$$

Now, note that $-Ku_K'=y_L$, and note the orthogonality of the y_j. Then, multiply $\ddot{\psi}$ by $dx\,u_K'$ and integrate to obtain

$$\int_{-\infty}^{\infty} dx\,u_K'\ddot{\psi}=-\text{const}\times\ddot{\alpha}_T(t)\ . \tag{3.29}$$

But since

$$-\ddot{\psi}=-c_0^2\frac{\partial^2\psi}{\partial x^2}+(3u_K^2-1)\psi+3u_K\psi^2+\psi^3\ ,$$

we have

$$\text{const}\times\ddot{X}=\int dx\,Ku_K'\left[-c_0^2\frac{\partial^2\psi}{\partial x^2}+(3u_K^2-1)\psi+3u_K\psi^2+\psi^3\right]\ , \tag{3.30}$$

which is the same as (3.24) if we set the constant to be equal to M_K and neglect the $\dot{X}$ and $\dot{X}^2$ terms. However, this theory is only good when $\alpha_T\ll 1$, so that $|X(t)-X(0)|<1$. So, for any nonstatic kink behavior, the Wada-Schrieffer theory of kink motion is not expected to be very useful.

IV. STATIC STRUCTURE OF THE KINK SYSTEM: THE POTENTIAL BARRIER

We have seen that the ϕ^4-lattice equation and its corresponding continuum analog both support solitary-wave kink solutions. Direct computations using the ϕ^4-lattice equation have indicated that moving kinks can slow down and become trapped; also the kink velocity shows an oscillatory variation. To understand fully these results one needs to consider the dynamics of kink-fluctuation interactions. It is useful, however, to first examine the potential energy of the system. As we will see, a central difference between a continuous and discrete system lies in the kink potential, for in the discrete system the potential varies periodically with the kink position. This gives rise ultimately to the velocity oscillation and trapping observed in simulations.

In the continuum description the Hamiltonian (1.4) of a static ϕ^4 kink becomes

$$E_K=\int_{-\infty}^{\infty}dx\left[\frac{c_0^2}{2}\left[\frac{\partial u}{\partial x}\right]^2+V_R(u)\right]_{u=u_K}=\frac{2(2c_0^2)^{1/2}}{3}\ , \tag{4.1}$$

which is manifestly translationally invariant. In a discrete lattice this symmetry is broken as the Hamiltonian of the static kink becomes

$$U(X)=\sum_l\left[\frac{c_0^2}{2}(u_{l+1}-u_l)^2+V_R(u_l)\right]_{u_l=u_K^l(X)}\ , \tag{4.2}$$

which now varies with the kink position X. As might be expected $U(X)$ is periodic in X; a typical variation over one period is shown in Fig. 8 as the "zeroth"-order solution. One sees that the potential minimum always occurs at a kink position midway between two lattice points, and the well depth depends upon the precise configuration used in the estimate of u_l.

Equation (4.2) is interpreted as the zeroth-order approximation to U, since $u_l=u_K^l$ implicitly assumes $\psi_l=0$ which satisfies (3.2). The continuum theory expressed in (3.8) can then be used to generate a perturbation series solution

$$u_l=u_K^l+\psi_l^{(1)}+\psi_l^{(2)}+\cdots\ , \tag{4.3}$$

where the $\psi_l^{(j)}$ are calculated from the perturbation theory of Sec. II, with the only change being that the kink structure function $F_K(x-X)$ is a nonhomogeneous term that causes ψ to be nontrivial. The first-order correction to the energy is shown in Fig. 8. Higher-order results should converge to the points in the figure which are the energy minima numerically obtained subject to (3.2). We represent the static lattice solution as

$$u_s^l(X)=u_K^l(X)+\psi_s^l(X)\ , \tag{4.4}$$

which yields a static Hamiltonian

$$H_S=\sum_l\left[\frac{c_0^2}{2}(u_s^{l+1}-u_s^l)^2+V_R(u_s^l)\right]\equiv U_S(X)\ . \tag{4.5}$$

Equation (4.5) can be reasonably well represented as

$$U_S(X)\simeq U_0+\frac{E_a}{2}\cos(2\pi X)\ . \tag{4.6}$$

The accuracy of this cosine fit increases with increasing C. Also shown in Fig. 8 is the continuum approximation (4.1)

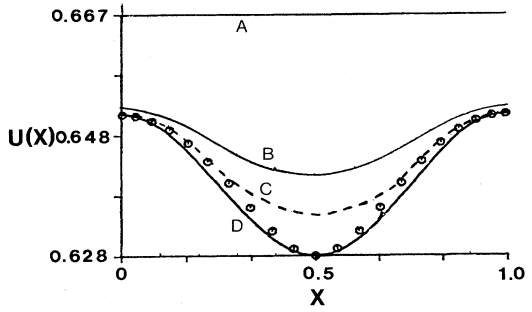

FIG. 8. Static kink potential $U(X)$ for $C=0.5$. A is the continuum approximation which is translationally invariant; B is the zeroth-order calculation from (4.5) with $\psi_e(X)=0$; the dashed curve C is the first-order perturbation calculation where $\psi_e(X)$ is determined from the static form of (3.17); D is the cosine fit to the circles which obtained from the minimum energy solution of (3.3) subject to (3.2) and static conditions. The circles, therefore, represent "exact" energies of the static lattice kink.

which is a constant and somewhat larger than U obtained by the perturbation or numerical approaches. It is clear that the periodic structure in the kink potential is a consequence of discrete lattice effects, effects completely absent in the traditional continuum approximation.

The well depth E_a has been determined numerically for various values of the parameter C. The results are shown in Fig. 9. The data are seen to extrapolate in the limit of small C to E_0, the double-well potential barrier (cf. Fig. 1), and at $C<2$ the variation is essentially exponential

$$E_a = E_0 \exp(-\alpha C) \tag{4.7}$$

with $\alpha = 4.84$. Equation (4.7) states that the barrier for kink motion is lower than the barrier for individual particle hopping from one minimum to the other of the potential $V_R(u)$ in (1.2). A general implication is that the presence of a kink has a "tunneling" effect on the particle motions[22]; it is a classical mechanism which increases the rate of transition or hopping between stable states. Also, one can make an analogy between kinks and dislocations in solids, and interpret E_a as the Peierl's barrier for dislocation motion. The Peierl's stress then becomes the maximum value of $-\partial U/\partial X$ or $\sigma_P = \pi E_a/b$.

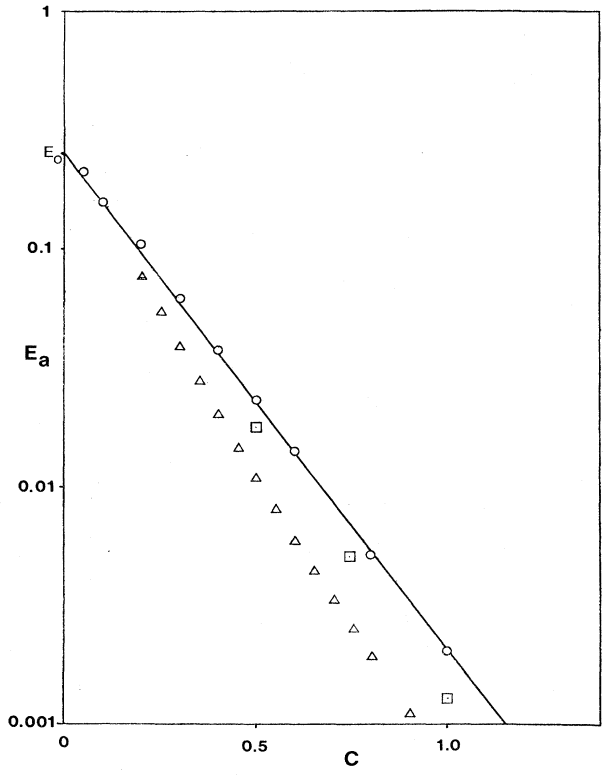

FIG. 9. Log plot of the kink energy barrier E_a as a function of C. The circles are the "exact" numerical solutions fit by the solid line $E_0\exp(-4.84C)$. The triangles and squares are the values obtained from the zeroth- and first-order-perturbation calculations, respectively.

V. DYNAMICAL STRUCTURE OF KINK SYSTEMS

A. Lattice trapping and velocity oscillations

The existence of a periodic potential $U(X)$ in the discrete lattice description makes it reasonable to expect that kink propagation will reflect features of this potential. The effects which we have noted in Sec. II are the slowing down of kink propagation, oscillations in the kink velocity during slowing down, and trapping of the kink when its velocity has reached a certain value. We will first analyze the process of lattice trapping and kink oscillation in the absence of damping, i.e., under the assumption that the kink conserves energy.

Let us relax the assumption that the system is static, but allow time dependence to appear through $X(t)$ only. Since the total Hamiltonian is conservative then the last assumption is equivalent to the statement that kinks must be conservative. The concept of the kink is expanded to include lattice solutions of the type (4.4) which vary with X only. Hamiltonian (1.4) with (4.4) then becomes

$$H_S = \sum_l \frac{(\dot{u}_s^l)^2}{2} + U_S(X) , \tag{5.1}$$

where

$$\dot{u}_s^l = -K \frac{\partial u_s^l}{\partial X} \dot{X} \tag{5.2}$$

and U_S is defined by (4.5). If we define the static kink mass as

$$M_S \equiv \sum_l K^2 \left[\frac{\partial u_s^l}{\partial X} \right]^2 \tag{5.3}$$

then (5.1)—(5.3) yield

$$H_S = \tfrac{1}{2} M_S \dot{X}^2 + U_S(X) . \tag{5.4}$$

In the continuum description

$$M_S \rightarrow \int_{-\infty}^{\infty} dx\, K^2 \left[\frac{\partial u_K}{\partial X} \right]^2 = M_K . \tag{5.5}$$

Notice that M_K is a constant whereas M_S has a periodic structure like U:

$$M_S \simeq M_0 + \frac{\delta M}{2} \cos(2\pi X) . \tag{5.6}$$

It turns out that M_0 is slightly smaller than M_K; as shown in Fig. 10 δM decreases with increasing C like a power law. If it is assumed that $M_S = M_0$, the conservative kink assumption

$$\frac{dH_S}{dt} = 0 \tag{5.7}$$

applied to (5.4) leads to

$$M_0 \ddot{X} = -\frac{\partial U_S}{\partial X} . \tag{5.8}$$

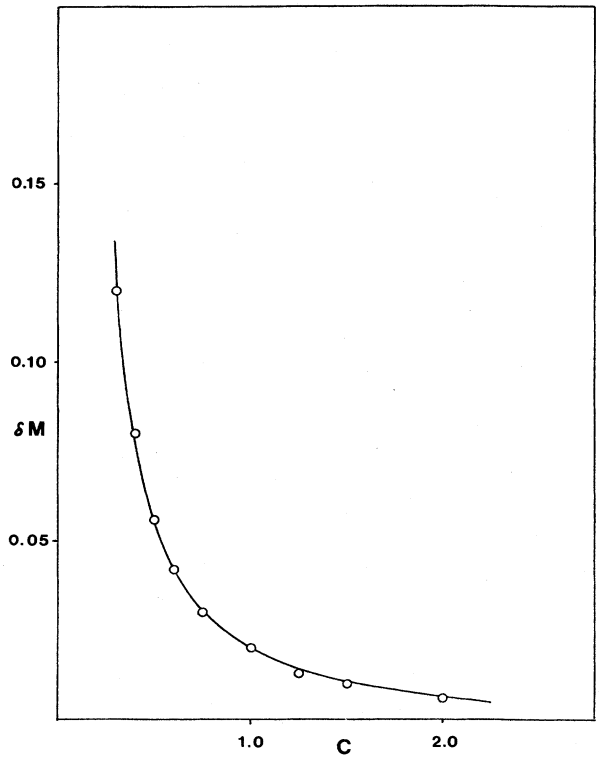

FIG. 10. Deviation δM from the mean value M_0 as a function of C. Solid curve is the power law $0.02C^{-3/2}$.

By letting U be represented by (4.6), one can integrate (5.8) to obtain

$$V(t)=V_K+\frac{\pi E_a}{M_0}\int_0^t dt'\sin[2\pi X(t')] , \tag{5.9}$$

where V_K is the initial kink velocity. To see the behavior of $V(t)$ at short times, we assume the accelerations are weak so that

$$X(t)\simeq X_0+V_K t . \tag{5.10}$$

Then

$$V(t)\simeq V_K+\frac{\pi E_a}{M_0\omega_K}\cos(\omega_K t+2\pi X_0) , \tag{5.11}$$

with $\omega_K=2\pi V_K$. The result shows that a periodic potential gives rise to oscillations in the velocity of a propagating kink.

The approximation (5.10) is only good when $(M_0V_K^2)/2 \gg E_a$. If $(M_0V_K^2)/2 \ll E_a$, then the kink will be unable to surmount the kink energy barrier and will become trapped. In this case it will oscillate about an average position X_0 where $U(X)$ has a minimum. One can describe this situation by an expansion

$$U(X)\simeq U(X_0)+\tfrac{1}{2}(X-X_0)^2\left.\frac{\partial^2 U}{\partial X^2}\right|_{X=X_0} . \tag{5.12}$$

Then (5.8) yields

$$V(t)=A_K\sin(\tilde{\omega}_0 t+\phi_0) , \tag{5.13}$$

where the amplitude A_K and phase ϕ_0 are constants yet to be determined, and

$$\tilde{\omega}_0=(2\pi^2 E_a/M_0)^{1/2} . \tag{5.14}$$

Equations (5.11) and (5.13) specify the kink-velocity oscillation frequency when the kink is propagating and when it is trapped. As a test of these predictions of the oscillation frequencies we show in Tables I and II comparisons of the theoretical values with numerical solution results.

The oscillation frequency of a propagating kink is predicted to vary directly with the initial velocity; this behavior can be seen in Table I. Reasonable agreement between the theory and simulation exists in Table II. The theory yields frequencies that are too low for low C values, which is expected since the actual kink potential $U(X)$ is softer than the approximate form (4.6) used to obtain (5.14). From an overall standpoint the conservative kink model described here appears to give at least a semiquantitative account of the numerical solution data. These features of velocity oscillation and trapping, of course, are entirely absent in the conventional continuum description.

B. Dissipative kink motions: Phonon radiation

Thus far only lattice motions associated with the translation of the lattice kink have been considered. This restriction eliminates dissipative effects since the kink system is then conservative. We now relax this assumption by writing the fluctuation amplitude as

$$\psi_l(t)=\psi_s^l(X(t))+\xi_l(t) , \tag{5.15}$$

where $\psi_s^l(t)$ is associated with the kink motion and $\xi_l(t)$ may be regarded as a radiation amplitude. Corresponding to this decomposition the Hamiltonian becomes

$$H=H_S(\dot{u}_s,u_s^l)+H_{S\xi}(\dot{u}_s^l,u_s^l;\dot{\xi}_l,\xi_l)+H_\xi(\dot{\xi}_l,\xi_l) , \tag{5.16}$$

where H_S describes the kink, $H_{S\xi}$ describes the kink-phonon interaction, and H_ξ the phonon (radiation) field. Notice that since $H=$const (the total system is conservative) then

$$\frac{dH_S}{dt}=-\frac{d}{dt}(H_{S\xi}+H_\xi) . \tag{5.17}$$

Thus, (5.16) and (5.17) allow for the exchange of energy between the kink and phonons. The conservative kink assumption,

TABLE I. Velocity oscillation frequencies of propagating kinks. Theoretical values are from $\omega_K=2\pi V$.

C	$\omega_K/2\pi$ (simulation)	$\omega_K/2\pi$ (theory)
2.0	0.45±0.01	0.468
1.0	0.25±0.01	0.255
1.0	0.24±0.01	0.249
0.9	0.24±0.01	0.250

TABLE II. Velocity oscillation frequencies of trapped kinks. Theoretical values are from Eq. (5.14), $M_0=M_K$.

C	$\tilde{\omega}_0$ (simulation)	$(2\pi^2 E_a/M_K)^{1/2}$
0.10	1.26	1.02
0.20	1.02	0.94
0.50	0.63	0.57
1.00	0.19	0.20
2.00	0.026	0.022

$$\frac{dH_S}{dt}=0\ , \tag{5.18}$$

decouples the kinks and phonons. Thus, the coupled kink-phonon system [which generally is the realized behavior of (1.4)] can give rise to dissipative effects, kink scattering effects, and other effects of the kink-phonon interaction.

In fact, by treating the right-hand side of (5.17) as the Rayleigh dissipative function[26] one can define a friction coefficient,

$$\Gamma(t)=\frac{1}{V^2}\frac{d}{dt}(H_{S\xi}+H_\xi)\ . \tag{5.19}$$

In general Γ is time dependent, and is related to the $\lambda(t)$ in (3.10). But numerical solutions show that the kink velocity may be represented as

$$V(t)\simeq V(0)e^{-\Gamma_0 t}\ , \tag{5.20}$$

plus an oscillatory component which may be treated as a perturbation to (5.20). The friction constant Γ_0 obtained in this manner behaves like

$$\Gamma_0=\begin{cases}\kappa e^{-\beta C}, & V>c_K\\ \sim 0, & V<c_K\end{cases} \tag{5.21}$$

with $\kappa=5.3$ and $\beta=7.5$, for $0.5<C<2$, so long as V is small compared to the sound velocity c_0. c_K is the transition velocity defined below. At higher velocities nonlinear effects represented by the $\dot{X}^2$ term in (3.10) cannot be ignored. If (5.21) can be extended to large C (where the damping was so small as to be difficult to measure) the damping will vanish in the continuum limit. Thus these empirical results strongly suggest that Γ_0, and thus kink damping, is associated with discrete lattice effects only. If this is true, such phenomena as kink diffusion in a thermal lattice cannot be predicted by a traditional continuum approach as the diffusion constant will diverge in the absence of systematic dissipation.

The numerical results indicate that a kink propagates at high velocity with dissipation but at low velocity its motion is nearly conservative. The transition from one behavior to the other is quite distinct, as can be seen in Fig. 11. The critical velocity where the transition occurs, denoted as c_K, is found to be independent of the initial velocity. Figure 12 shows the variation of c_K with C.

When dissipation is included, Eq. (5.8) must be modified. We make the phenomenological assumption that the damping term $\lambda\dot{X}$ in (3.10) can be represented by $\Gamma_0\dot{X}M_0$,

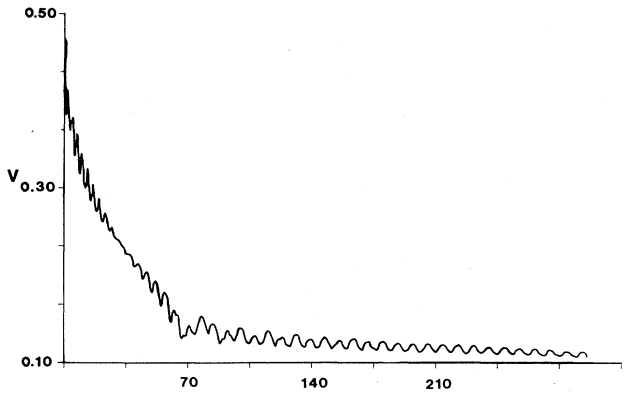

FIG. 11. Velocity transition from strongly damped to weakly damped motion for the case $C=0.8$, $V(0)=0.50$. The transition velocity c_K in this case occurs at roughly $V=0.15$. Oscillations are due to lattice discreteness [see Eq. (5.11)].

so that we may write

$$\ddot{X}(t)+\Gamma_0\dot{X}(t)=-\frac{1}{M_0}\frac{\partial U}{\partial X}\ . \tag{5.22}$$

Integrating once gives

$$V(t)=e^{-\Gamma_0 t}\left[V_K+\frac{\pi E_a}{M_0}\int_0^t dt'\,e^{\Gamma_0 t'}\sin[2\pi X(t')]\right]\ . \tag{5.23}$$

As a test of this model we have numerically evaluated the integral (5.23) using the $X(t)$ data generated from the numerical solutions. The results for $V(t)$ obtained thereby are compared with the direct numerical solution of (2.2) subject to (3.2) which incorporates kink-phonon effects exactly (see Figs. 13–16). The phenomenological theory is seen to be adequate at intermediate and large-C values, $C\gtrsim 0.75$, particularly at short times. In addition to oscillations in the propagating regime, trapping, and dissipation are also reproduced. The apparently undamped oscillation in Fig. 16 indicates that Γ_0 is effectively zero at

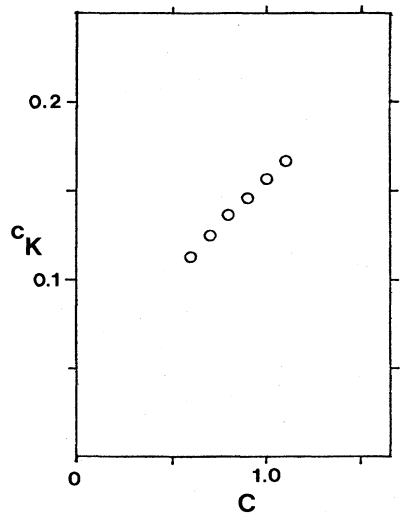

FIG. 12. Transition velocity c_K vs C.

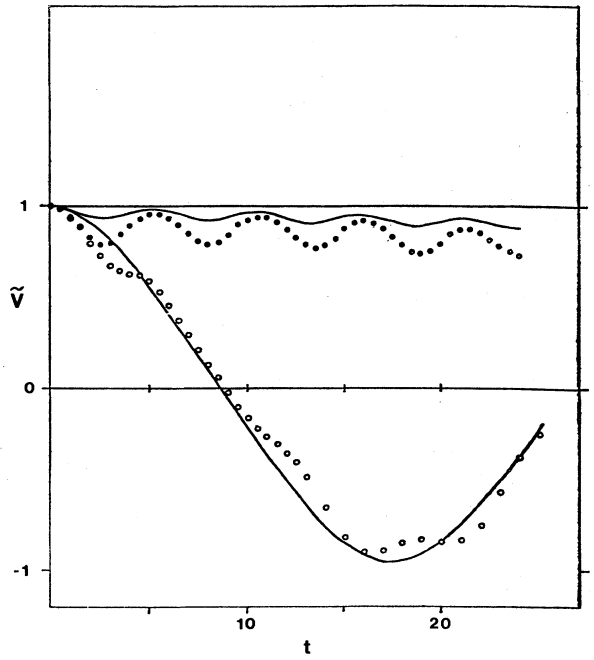

FIG. 13. Reduced kink velocity $\tilde{V}=V/V(0)$ for $C=1$. The circles are values obtained from a numerical integration of (2.1); the curves are from (5.23) using the $X(t)$ data so generated. The solid circles (●) are for $V(0)=0.2$; the open circles (○) are for $V(0)=0.04$. Velocities are characteristic of damped oscillatory propagation, and trapped oscillatory motions, respectively. For comparison, the constant-velocity continuum solution is shown at $\tilde{V}=1$.

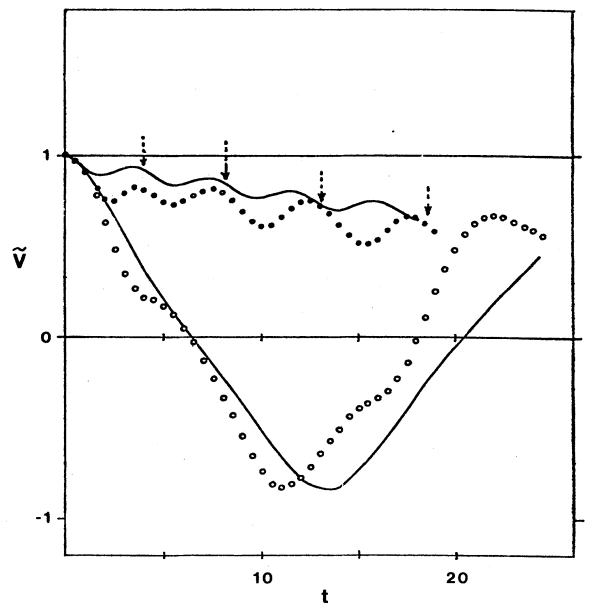

FIG. 14. Same as Fig. 13 for $C=0.75$. Solid circles are for $V(0)=0.3$; open circles are for $V(0)=0.1$.

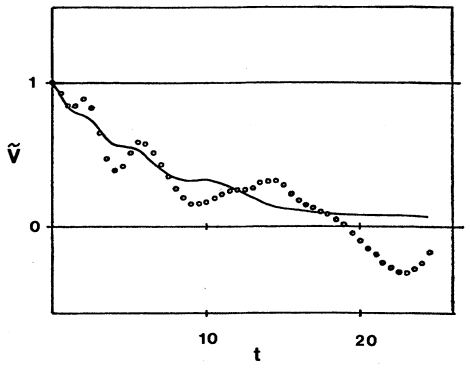

FIG. 15. Same as Fig. 13 for $C=0.5$, except that a distinct propagating oscillatory velocity was not observed at any velocity; only strong damping followed by trapping of the kink is found. In this case $V(0)=0.5$.

$C=0.5$, a property which was not incorporated in the phenomenological calculation.

In summary, kinks are found to move freely in a lattice only for large C ($\gg 1$) where the field kink solution is a good approximation. Atomistic effects of the lattice give rise to two distinct regimes of kink motions: a propagating regime and a nonpropagating (trapped) regime as indicated in Fig. 17. For a given value of C in the propagating regime, a distinct transition is present as the kink velocity passes through c_K. Similar transitions have been found in simulations of steady dislocation motion under shear stress in two and three dimensions.[27,28]

VI. CONCLUSION

We have found that discrete lattice effects are fundamental to a proper understanding of solitary-wave phe-

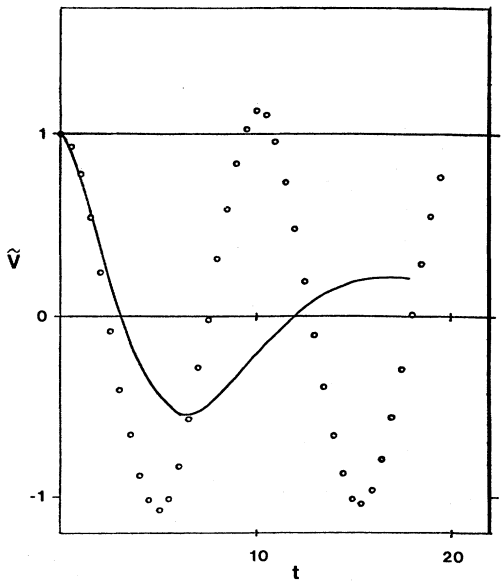

FIG. 16. Same as Fig. 15 for $V(0)=0.1$. There is little, if any dissipation, of kink motion.

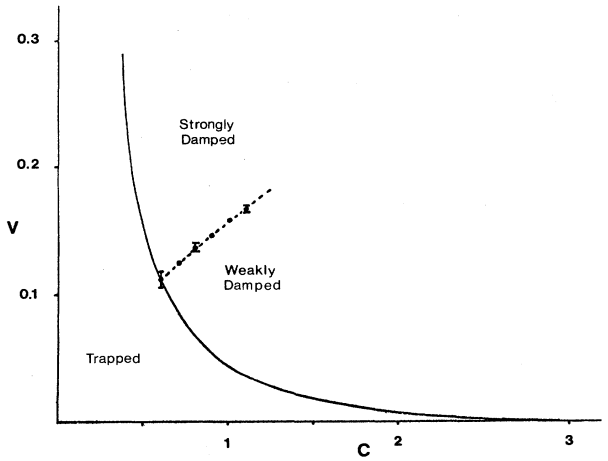

FIG. 17. Regime diagram of kink motion. The solid curve is $V=(2E_a/M_K)^{1/2}$, the theoretical boundary of the trapping regime. Numerical solutions confirm that below this boundary kinks becomes trapped and oscillate about a midlattice position; above the boundary they undergo damped oscillatory propagation. The dotted curve represents the transition velocity that distinguishes strongly and weakly damped motions for a given value of C. The data points are numerically determined values of c_K. As C increases the lattice effects of damping and trapping rapidly disappear. For $C>20$, the continuum approximation should be very accurate.

nomena observable away from the continuum limit. These effects include strong kink-phonon coupling which gives rise to dissipation, velocity oscillations, and lattice trapping of kinks. We have discovered that it is very useful to reformulate the N-body lattice problem as an $(N+1)$-body kink plus fluctuation problem, which is naturally amenable to a perturbative approach in kink-phonon coupling. The latter fact still remains to be fully exploited in the understanding of phonon radiation and dissipation of kink motion.

Our numerical results and phenomenological theory strongly suggest that the friction kinks feel in a conservative system is primarily due to discrete lattice effects. If dissipative effects do indeed exist in the continuous ϕ^4-field theory, as has been proposed by others,[8,16] they are relatively unimportant; single continuum kinks are essentially freely moving, even in the presence of fluctuations, in the absence of external forces.

Because of the periodic lattice kink potential, one expects that lattice motions of a kink in a thermal lattice at low temperatures would be an activation process. This point is treated in a subsequent paper by the authors. The results of the kink-fluctuation formalism justify a generalized Langevin model for the kink motions. It would be of great interest to numerically examine the properties of the kink equation of motion to see if the kink is a Brownian-type activated particle (which gives rise to a very simple diffusion coefficient). This would require a measurement of the correlations of thermal forces acting on the kink as well as the memory of the dissipative term. It is also of interest to understand the average kink structure as a function of velocity; e.g., does it contract in the lattice to the same degree as in the continuum theory, and what are the effects of thermal fluctuations on the effective width (and thus effective mass and formation energy)?

At present the dissipative effects and transitions in dissipation are not well understood. It is expected that with the aid of perturbation theory the mechanism for dissipation can be understood from the kink-fluctuation theory developed here. Already, some progress has been made in this direction.[24] Such studies may be aided by generalizing the Hamiltonian to include a simple external-field term linear in the displacement amplitudes. This would yield a nonhomogeneous equation of motion which may have simple but interesting solutions.[24]

Finally, one significant limitation of the present theory is that it treats only a single kink in one dimension. Multiple kink constraints need to be invoked which yield tractable equations of motion. When this is accomplished more can be understood about kink-kink interactions, and fluctuation behavior in a thermal lattice. Although one-dimensional treatments are useful in understanding such systems as polymer chains, two- and three-dimensional treatments may be of more value in understanding the continuum theory of dislocations, its limitations, and how it can be improved. The available continuum theory can be used as a reference state to develop the kink-fluctuation theory.

ACKNOWLEDGMENTS

This work was supported by the Army Research Office and the National Science Foundation.

APPENDIX

We begin with the equation of constraint (3.2) and its time derivative

$$\frac{d}{dt}\sum_l (u'_K)_l\psi_l=0\ , \tag{A1}$$

where

$$(u'_K)_l=\frac{1}{K}\frac{\partial u_K}{\partial X}\bigg|_{x=x_l}$$

This yields

$$\sum_l [-K\dot{X}(u''_K)_l\psi_l+(u'_K)_l\dot{\psi}_l]=0\ , \tag{A2}$$

but u_l and its time derivative can be written

$$u_l=u_K^l+\psi_l\ ,$$
$$\dot{u}_l=-K(u'_K)_l\dot{X}+\dot{\psi}_l\ ,$$

so

$$\dot{\psi}_l=\dot{u}_l+K\dot{X}(u'_K)_l\ . \tag{A3}$$

Then (A3) in (A2) yields

$$\left[\sum_l K^2[(u'_K)_l^2-(u''_K)\psi_l]\right]\dot{X}=-K\sum_l (u'_K)_l\dot{u}_l\ . \tag{A4}$$

Define an effective kink mass M by

$$M\equiv\sum_l K^2[(u'_K)^2-(u''_K)_l\psi_l] \tag{A5}$$

so that the kink momentum P becomes

$$P \equiv M\dot{X} = -\sum_l K(u'_K)_l \dot{u}_l \ . \tag{A6}$$

In this way the momentum of the kink can be extracted from the (nondimensional) momentum $\dot{u}_l$ of the particles. Newton's law for kink motion may be written down from the time derivative of (A6),

$$\frac{dP}{dt} = -K\frac{d}{dt}\sum_l (u'_K)_l \dot{u}_l$$

$$= -K\sum_l [-K\dot{X}(u''_K)_l \dot{u}_l + (u'_K)_l \ddot{u}_l] \ , \tag{A7}$$

but

$$\ddot{u}_l = -\frac{\partial U}{\partial u_l} \ , \tag{A8}$$

where U includes all potential terms. (A3) and (A8) can be used in (A7) to yield

$$\frac{dP}{dt} = -K\sum_l \left[-K\dot{X}(u''_K)_l [\dot{\psi}_l - K\dot{X}(u'_K)_l] - (u'_K)_l \frac{\partial U}{\partial u_l} \right]$$

$$= \left[\sum_l K^2 (u''_K)_l \dot{\psi}_l \right] \dot{X} - \left[\sum_l K^3 (u'_K u''_K)_l \right] \dot{X}^2$$

$$+ \sum_l K(u'_K)_l \frac{\partial U}{\partial u_l} \ . \tag{A9}$$

Now, note that

$$\frac{\partial U}{\partial X} = \sum_l \frac{\partial u_l}{\partial X}\frac{\partial U}{\partial u_l}$$

$$= \sum_l \frac{\partial u^l_K}{\partial X}\frac{\partial U}{\partial u_l} = -\sum_l K(u'_K)_l \frac{\partial U}{\partial u_l} \ . \tag{A10}$$

This is because $\partial/\partial X$ implicitly holds ψ_l constant as well as t. Thus (A9) can be rewritten as

$$\frac{dP}{dt} = \left[\sum_l K^2 (u''_K)_l \dot{\psi}_l \right] \dot{X} - \left[\sum_l K^3 (u'_K u''_K)_l \right] \dot{X}^2 - \frac{\partial U}{\partial X} \ . \tag{A11}$$

Now

$$\frac{dP}{dt} = \frac{d}{dt}(M\dot{X}) = M\ddot{X} + \dot{X}\frac{dM}{dt} \tag{A12}$$

and

$$\frac{dM}{dt} = \frac{d}{dt}\left[\sum_l K^2 (u'_K)_l^2 - \sum_l K^2 (u''_K)_l \psi_l \right]$$

$$= -2\left[\sum_l K^3 (u'_K u''_K)_l \right] \dot{X} - \left[\sum_l K^2 (u''_K)_l \dot{\psi}_l \right]$$

$$+ \left[\sum_l K^3 (u'''_K)_l \psi_l \right] \dot{X} \tag{A13}$$

so (A12) and (A13) in (A11) yield

$$M\ddot{X} + \left[-2\sum_l K^2 (u''_K)_l \dot{\psi}_l \right] \dot{X}$$

$$+ \left[-\sum_l K^3 (u'_K u''_K)_l + \sum_l K^3 (u'''_K)_l \psi_l \right] \dot{X}^2 = -\frac{\partial U}{\partial X} \ . \tag{A14}$$

The terms in large parentheses are just the values $\lambda(t)$ and $\xi(t)$ found in the text.

[1] W. Atkinson and N. Cabrera, Phys. Rev. A 138, 763 (1965).
[2] J. H. Weiner, Phys. Rev. A 136, 863 (1964).
[3] J. Frenkel and T. Kontorowa, Phys. Z. Sowjetunion 13, 1 (1938), and discussed in F. C. Frank and J. H. van der Merwe, Proc. R. Soc. London Ser. A 198, 216 (1949).
[4] J. A. Krumhansl and J. R. Schrieffer, Phys. Rev. B 11, 3535 (1975).
[5] T. Schneider and E. Stoll, Phys. Rev. Lett. 35, 296 (1975).
[6] T. Schneider and E. Stoll, Phys. Rev. B 13, 1216 (1975).
[7] T. Schneider and E. Stoll, Phys. Rev. B 17, 1302 (1978).
[8] G. F. Mazenko and P. S. Sahni, Phys. Rev. B 18, 6139 (1978).
[9] P. S. Sahni and G. F. Mazenko, Phys. Rev. B 20, 4674 (1979).
[10] J. F. Currie, S. E. Trullinger, A. R. Bishop, and J. A. Krumhansl, Phys. Rev. B 15, 5567 (1977).
[11] J. F. Currie, A. Blumen, M. A. Collins, and J. Ross, Phys. Rev. B 19, 3645 (1979).
[12] M. A. Collins, A. Blumen, J. F. Currie, and J. Ross, Phys. Rev. B 19, 3630 (1979).
[13] T. R. Koehler, A. R. Bishop, J. A. Krumhansl, and J. R. Schrieffer, Solid State Commun. 17, 1515 (1975).
[14] W. Hasenfratz and R. Klein, Physica 89A, 191 (1977).
[15] J. C. Kimball, Phys. Rev. B 21, 2104 (1980).
[16] Y. Wada and J. R. Schrieffer, Phys. Rev. B 18, 3897 (1978).
[17] W. C. Kerr, Phys. Rev. B 19, 5773 (1979).
[18] S. Aubry and R. Pick, Ferroelectrics 8, 471 (1974).
[19] S. Aubry, J. Chem. Phys. 62, 3217 (1975).
[20] S. Aubry, J. Chem. Phys. 64, 3392 (1976).
[21] R. Jackiw and J. R. Schrieffer, Nucl. Phys. B 190, 253 (1981).
[22] J. L. Skinner and P. G. Wolneys, J. Chem. Phys. 73, 4015 (1980).
[23] J. L. Skinner and P. G. Wolneys, J. Chem. Phys. 73, 4022 (1980).
[24] J. Andrew Combs, Ph.D. thesis, Department of Nuclear Engineering, Massachusetts Institute of Technology, 1981 (unpublished).
[25] E. Tomboulis, Phys. Rev. D 12, 1678 (1975).
[26] Herbert Goldstein, *Classical Mechanics*, 2nd ed. (Addison-Wesley, Reading, Mass., 1980), p. 24.
[27] W. F. Hartl and J. H. Weiner, Phys. Rev. 152, 634 (1966).
[28] W. G. Hoover, N. E. Hoover, and William C. Moss, J. Appl. Phys. 50, 829 (1979).